Ionization Energies of Atoms and Atomic Ions

Peter F. Lang and Barry C. Smith*

School of Biological and Chemical Sciences, Birkbeck College (University of London), Malet Street, London WC1E 7HX, England; *smithbc@talk21.com

The ionization energy of an atom depends on its atomic number and electronic configuration. Ionization energies tend to decrease on descending groups in the s and p blocks (with exceptions) and group 3 in the d block of the periodic table. Successive ionization energies increase with increasing charge on the cation. This paper describes some less familiar aspects of ionization energies of atoms and atomic ions. Apparently irregular first and second ionization energies of transition metals and rare earth metals are explained in terms of the electronic configurations of the ground states. A semiquantitative treatment of pairing, exchange, and orbital energies accounts for discontinuities at half-filled p, d, and f electron shells and the resulting zigzag patterns.

We begin with a reminder of the difference between ionization potential and ionization energy. Ionization potential is the electric potential (measured in volts) required to separate an electron from the orbital system in free space with the kinetic energy remaining unchanged. Ionization energy is the work done in removing the electron at zero temperature and is measured conveniently in electronvolts, where 1 eV = 1.6022×10^{-19} J. The molar ionization energy, or change in molar internal energy, is N_A eV = 96.485 kJ mol^{-1} where N_A is the Avogadro constant.

Ionization wavenumbers (reciprocal wavelengths) are derived from series limits of atomic spectral lines. The energy per cm^{-1} is 1.2398×10^{-4} eV or 1.9864×10^{-23} J. The molar energy per cm^{-1} is 11.962 J mol^{-1}.

Sources of Data

Three volumes containing wavenumbers and atomic energy levels *(1)* preceded the critical survey by Moore of ionization limits from ground state to ground state for atoms and atomic ions. Ionization energies derived from optical and mass spectroscopy and calculations ranging from crude approximations to complex equations based on quantum mechanical theory are accompanied by assessments of reliability and a bibliography *(2)*. Martin, Zalubus, and Hagan reviewed energy levels and ionization limits for rare earth elements *(3)*. *Handbook of Chemistry and Physics (4)* contains authoritative data from these and later sources. For example, an experimental value for the second ionization energy of cesium, 23.157 eV *(5)*, supersedes 25.1 eV *(2)*.

Periodicity

Third ionization energies of atoms from lithium (Z = 3) to hafnium (Z = 72) are plotted against atomic number, Z, in Figure 1. Values are from reference *(4)* except those for Cs (Z = 55) and Ba (Z = 56) from the *Journal of the Optical Society of America (5, 6)*. The first peak occurs at Be^{2+} (Z = 4), which has the electronic configuration $1s^2$. Peaks corresponding to filled s, p, d, f, and half-filled d and f orbitals illustrate the shell model of the atom *(7)*. Figure 1 provides a more compelling demonstration of periodicity than plots of first ionization energy *(8)* where transition metals and rare earth metals do not show zigzag patterns.

For M^{2+} ions, 3d orbitals have lower energies than 4s orbitals *(9)*, 4d orbitals have lower energies than 5s orbitals, and 5p orbitals have lower energies than 4f orbitals.

s Electrons

Figure 2 shows how first ionization energies decrease from hydrogen to cesium and from helium to barium. Straight lines joining ionization energies from five pairs of group 1 and 2 atoms have intercepts of approximately 2.6

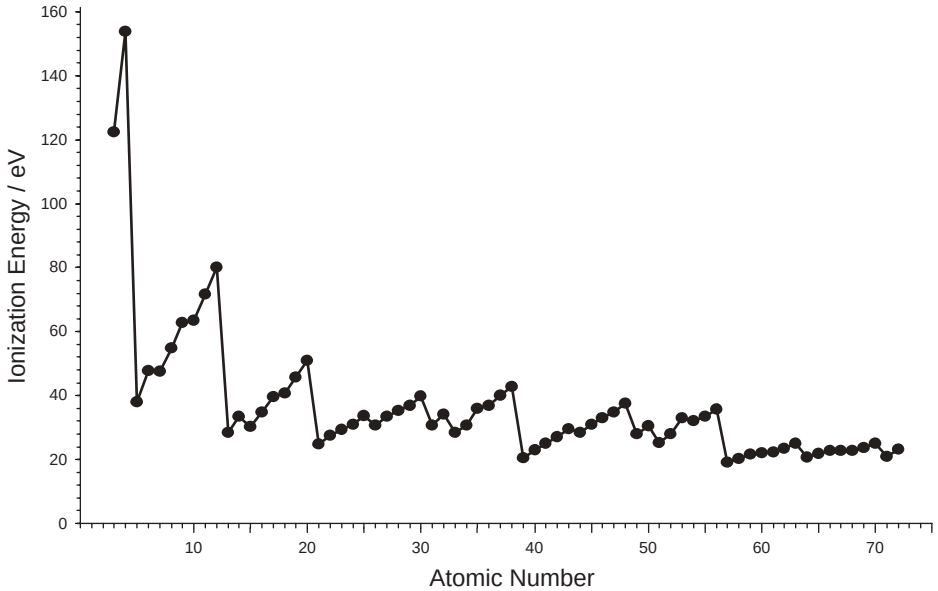

Figure 1. Third ionization energies from lithium to hafnium.

eV. The intercept for lithium and beryllium is 1.46 eV but there is no reason to believe that the Moore values are incorrect. First ionization energies of francium and radium, not shown in Figure 2, are greater than those of cesium and barium respectively as a result of poor shielding by 4f electrons.

First ionization energies of atoms from hydrogen to beryllium are plotted in Figure 3. The ionization energy of helium is greater than that of hydrogen but less than four times as great *(10)* because the electrons provide some screening for each other as mutual repulsion pushes them away from the nucleus. The outer electron of lithium occupies a new shell screened by two electrons and the ionization energy is lower than that of hydrogen or helium. Similarly, the first ionization energy of beryllium is higher than that of lithium but much lower than that of helium. Second ionization energies from helium to boron are higher and follow a similar pattern. Other points correspond to third, fourth, and fifth ionization energies of the respective atoms.

Ionization energies of atomic hydrogen and one-electron atomic ions, at the left of Figure 3, are approximately proportional to the electron–nucleus attraction, Z^2. They are reproduced with reasonable accuracy by the following expression, where R_M is the appropriate Rydberg constant and α is the Sommerfeld fine structure constant *(11)*:

$$R_M Z^2 \left[1 + Z(Z-1)\frac{\alpha^2}{4}\right]$$

Screening (electron–electron repulsion) reduces electron–nucleus attractions in helium and two-electron atomic ions but ionization energies are not functions of simple squares, $(Z - S)^2$, where S is a screening constant *(12)*. The correct expression takes account of relaxation by the remaining electron *(13)*:

$$Z^2 - \frac{5Z}{4} + \frac{5}{16}$$

The square roots of the first ionization energies plotted against atomic number for six isoelectronic series are shown in Figure 4. The one-electron plot falls close to a straight line through the origin. Differences between square roots of successive ionization energies for the other series confirm increasing curvature from left to right. Gradients for 2s series approach one half and gradients for 3s series approach one third of the gradient for the one-electron series. Their ionization energies are based on quadratic expressions, where n is the principal quantum number of the electron, and b and c are constants characteristic of the series:

$$\left(\frac{Z}{n}\right)^2 - bZ + c$$

p Electrons

First ionization energies of atoms from the first three periods of groups 13 to 18 (2p, 3p, and 4p electron series) form zigzag patterns in Figure 5. First and second ionization energies of atoms from the next two periods (5p and 6p series) appear in Figure 6. Gallium has a slightly higher first ionization energy than aluminum because of relatively poor

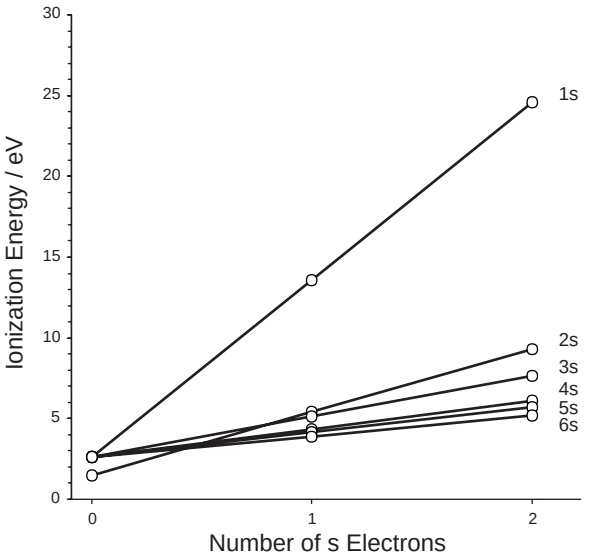

Figure 2. First ionization energies of group 1 and group 2 atoms.

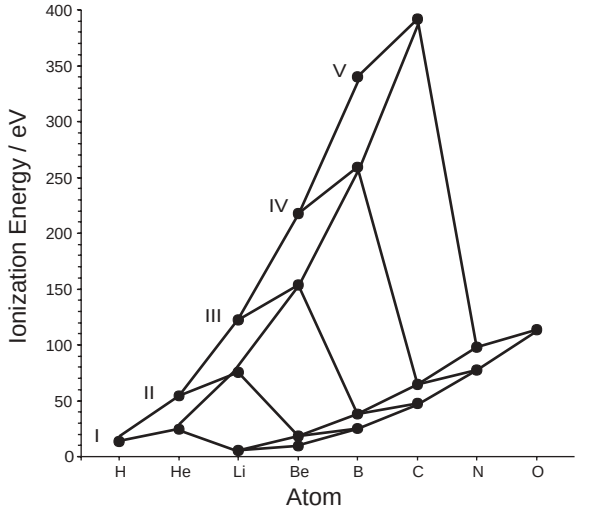

Figure 3. Energies to remove 1s or 2s electrons from atoms or ions. Roman numerals denote the ionization number.

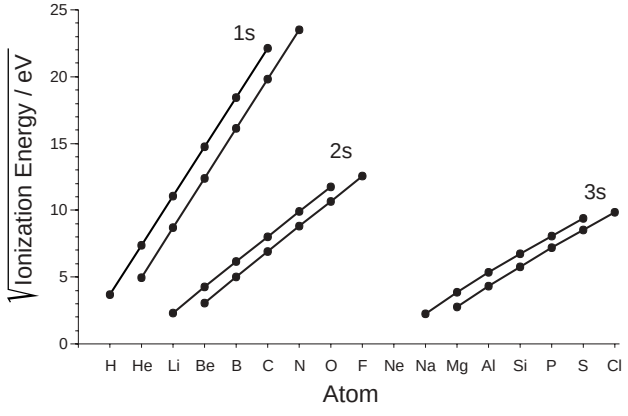

Figure 4. Square roots of energies to remove 1s, 2s, or 3s electrons.

shielding by 3d electrons. Thallium and lead have higher first ionization energies than indium and tin, respectively, because of poor shielding by 4f electrons. First ionization energies vary in the order B > Al < Ga > In < Tl and C > Si > Ge > Sn < Pb but decrease with increasing atomic number down groups 15 to 18. Lead and bismuth have greater second ionization energies than tin and antimony respectively.

The first ionization energy of bismuth appears to be anomalous. The increase from thallium to lead is followed by a decrease to bismuth rather than the expected increase to approximately 8 eV *(14)*. It has been claimed that spin–orbit coupling by the Russell–Saunders scheme would lower the ground state of Bi^+ by 0.8 eV and that the lower ionization energy is correct *(15)*. Condon and Shortley identified differences between theoretical and experimental values for a number of atoms *(16)* but spin–orbit coupling effects of this magnitude were not observed.

First ionization energies at the bottom of Figure 7 increase from boron to nitrogen, decrease to oxygen, and increase to neon. Second ionization energies increase from carbon to oxygen, decrease to fluorine, and increase to sodium. Third, fourth, and fifth ionization energies of the respective atoms show similar patterns.

Discontinuities at half-filled p orbitals are conventionally attributed to repulsion between electrons of opposite spin occupying the same orbital in the second half of a subperiod.

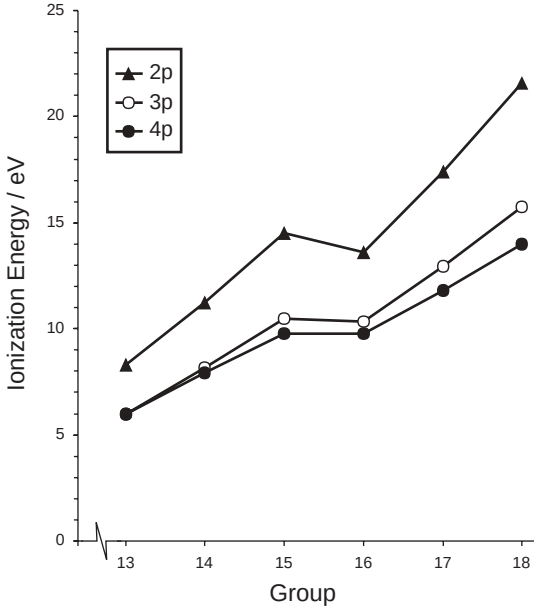

Figure 5. Energies to remove first p electron.

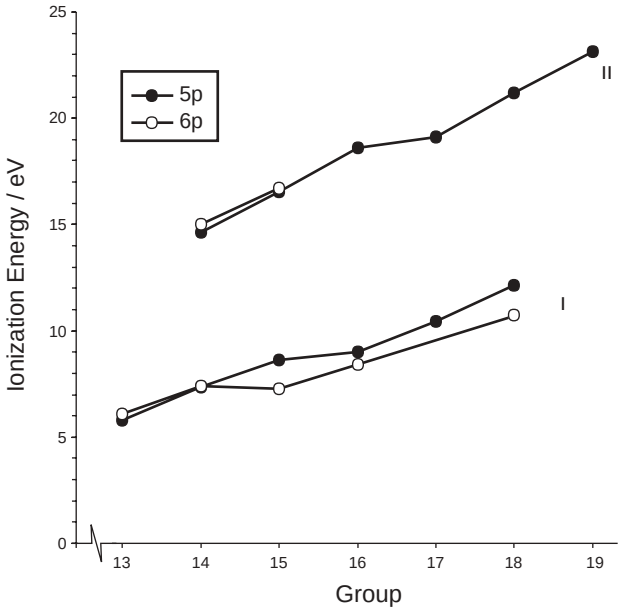

Figure 6. Energies to remove first and second p electrons. Roman numerals denote the ionization number.

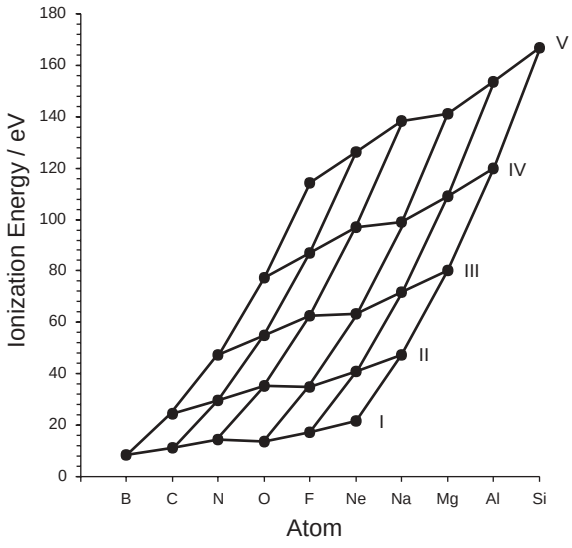

Figure 7. Energies to remove 2p electrons. Roman numerals denote the ionization number.

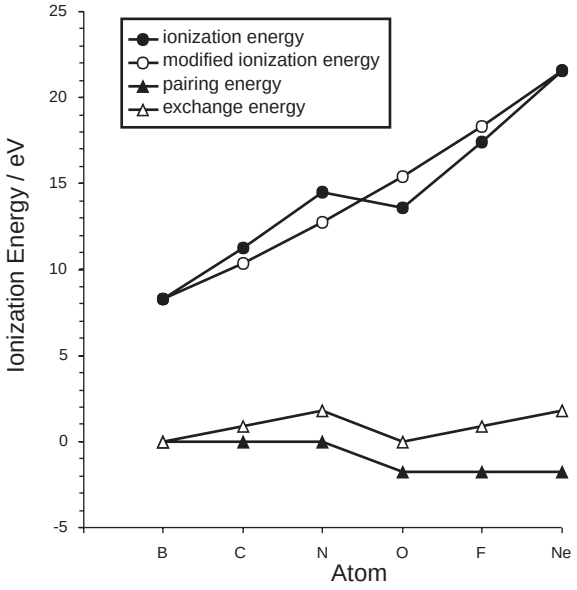

Figure 8. First ionization energies from boron to neon.

Less attention has been paid to quantum mechanical exchange interactions, where more energy is required to ionize an electron in a group with parallel spins as a result of increased electron–nuclear attractions *(17)*. The semiquantitative approach developed here considers double occupancy and exchange interactions as discussed by Blake *(18)* and takes account of the work of Johnson *(19)* and Cann *(20)*.

Table 1 summarizes numbers of pairing interactions (pairs of electrons occupying the same orbital), p_0 and p_1 (subcripts denote ionization numbers); numbers of exchange interactions between pairs of electrons having parallel spins, e_0 and e_1; and changes on ionization, Δp and Δe, for boron to neon and their singly charged cations. We assume that individual pairing energies, P, and exchange energies, E_{ex}, are constant across the subperiod. Figure 8 shows how ionization energies from boron to neon are lowered by changes in pairing energy, $P\Delta p$, and raised by changes in exchange energy, $E_{ex}\Delta e$, where $P = -2E_{ex} = 1.778$ eV. Modified ionization energies, adjusted for pairing and exchange interactions, lie on a curve that increases smoothly from boron to neon. Modified second ionization energies produce a curve that increases from carbon through oxygen and fluorine to sodium, where $P = -2E_{ex} = 2.354$ eV.

Similar curves can be derived for other p electron series, where $P = -2E_{ex} = 1.038$ eV for first ionization energies from aluminum to argon and $P = -2E_{ex} = 0.784$ eV for first ionization energies from gallium to krypton.

Transition Metals

First ionization energies of calcium, strontium, barium, and transition metals are plotted against group number in Figure 9. Apparent irregularities across the periods *(21)* are caused by different ground-state electronic configurations *(1)* that are summarized in Table 2. Hafnium and other post-lanthanum atoms have higher first ionization energies than

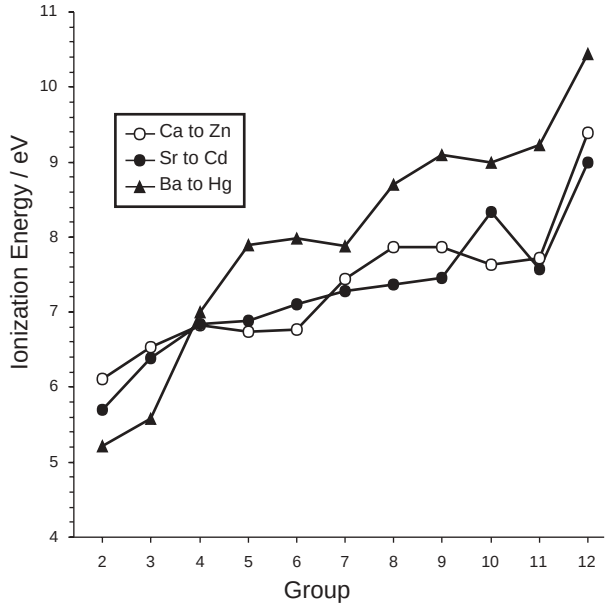

Figure 9. First ionization energies of alkaline earth and transition metals.

Table 1. Pairing and Exchange Interactions on Ionization of Atomic Boron to Neon

Atom	p_0	e_0	Ion	p_1	e_1	Δp	Δe
B	0	0	B^+	0	0	0	0
C	0	1	C^+	0	0	0	-1
N	0	3	N^+	0	1	0	-2
O	1	3	O^+	0	3	-1	0
F	2	4	F^+	1	3	-1	-1
Ne	3	6	Ne^+	2	4	-1	-2

Table 2. Ground State Electronic Configurations of Transition-Metal Atoms and Ions

Z	Atom	n	M		M^+		M^{2+}		M^{3+}	
			3d	4s	3d	4s	3d	4s	3d	4s
20	Ca	0	0	2	0	1	0	0		
21	Sc	1	1	2	1	1	1	0	0	0
22	Ti	2	2	2	2	1	2	0	1	0
23	V	3	3	2	4	0	3	0	2	0
24	Cr	4	5	1	5	0	4	0	3	0
25	Mn	5	5	2	5	1	5	0	4	0
26	Fe	6	6	2	6	1	6	0	5	0
27	Co	7	7	2	8	0	7	0	6	0
28	Ni	8	8	2	9	0	8	0	7	0
29	Cu	9	10	1	10	0	9	0	8	0
30	Zn	10	10	2	10	1	10	0	9	0
			4d	5s	4d	5s	4d	5s	4d	5s
38	Sr	0	0	2	0	1	0	0		
39	Y	1	1	2	0	2	0	1	0	0
40	Zr	2	2	2	2	1	2	0	1	0
41	Nb	3	4	1	4	0	3	0	2	0
42	Mo	4	5	1	5	0	4	0	3	0
43	Tc	5	5	2	5	1	5	0	4	0
44	Ru	6	7	1	7	0	6	0	5	0
45	Rh	7	8	1	8	0	7	0	6	0
46	Pd	8	10	0	9	0	8	0	7	0
47	Ag	9	10	1	10	0	9	0	8	0
48	Cd	10	10	2	10	1	10	0	9	0
			5d	6s	5d	6s	5d	6s	5d	6s
56	Ba	0	0	2	0	1	0	0		
57	La	1	1	2	2	0	1	0	0	0
72	Hf	2	2	2	1	2	2	0	1	0
73	Ta	3	3	2	4	0				
74	W	4	4	2	5	0				
75	Re	5	5	2	5	1				
76	Os	6	6	2	6	1				
77	Ir	7	7	2	8	0				
78	Pt	8	9	1	9	0	8	0	7	0
79	Au	9	10	1	10	0	9	0	8	0
80	Hg	10	10	2	10	1	10	0	9	0

corresponding atoms in the first and second periods, presumably because of poor shielding by 4f electrons. Observed ionization energies from ground state to ground state *(4)* will appear as filled circles in Figures 10–12. Other symbols represent ionization energies derived from wavenumbers of excited states *(1)*.

First Transition Period

Most atoms in the first transition period have outer electronic configurations $M(3d^n4s^2)$, where n represents the position of the atom in the d block. First and second ionization energies are examined in Figure 10. Calcium, scandium, titanium, manganese, iron, and zinc lose both s electrons in processes $M(3d^n4s^2) \rightarrow M^+(3d^n4s^1) \rightarrow M^{2+}(3d^n4s^0)$. Their ionization energies, with energies derived from wavenumbers of excited states for other atoms *(1)*, fall on curves IA and IIA. Chromium ($n = 4$) and copper ($n = 9$) lose one s electron in the process $M(3d^{n+1}4s^1) \rightarrow M^+(3d^{n+1}4s^0)$ and their first ionization energies form part of curve IB, which is slightly lower than curve IA. Vanadium, cobalt, and nickel lose two s electrons and gain one d electron in processes $M(3d^n4s^2) \rightarrow M^+(3d^{n+1}4s^0)$. Their first ionization energies form part of zigzag pattern IC, which has a minimum at chromium and a maximum at manganese. This is the reverse of zigzag pattern IIB formed by second ionization energies of atoms that lose one d electron in the process $M^+(3d^{n+1}4s^0) \rightarrow M^{2+}(3d^n4s^0)$ and where chromium is higher than manganese. Zinc ($n = 10$) can not contain more than ten 3d electrons and does not form part of curve IB or zigzag patterns IC or IIB.

Third ionization energies from Figure 1 are plotted on a larger scale in Figure 11. The systematic loss of one d electron in the process $M^{2+}(3d^n4s^0) \rightarrow M^{3+}(3d^{n-1}4s^0)$ gives a zigzag pattern that excludes calcium ($Z = 20$, $n = 0$), increases from scandium to manganese, decreases to iron, and increases to zinc. As with p electrons, discontinuities are conventionally attributed to repulsion between paired electrons of opposite spin in the second half of the subperiod. The energy of removal of d electrons was discussed by Catalan et al. in 1954 *(22)*. Our semiquantitative approach involves pairing and exchange energies as before and incorporates orbital energies *(19, 20, 23)*.

Table 3. Pairing and Exchange Interactions and Term Symbols for Ions of the First Transition Period

Ion	p_2	e_2	Term	Ion	p_3	e_3	Term	Δp	Δe
Sc^{2+}	0	0	^2D	Sc^{3+}	0	0	^1S	0	0
Ti^{2+}	0	1	^3F	Ti^{3+}	0	0	^2D	0	−1
V^{2+}	0	3	^4F	V^{3+}	0	1	^3F	0	−2
Cr^{2+}	0	6	^5D	Cr^{3+}	0	3	^4F	0	−3
Mn^{2+}	0	10	^6S	Mn^{3+}	0	6	^5D	0	−4
Fe^{2+}	1	10	^5D	Fe^{3+}	0	10	^6S	−1	0
Co^{2+}	2	11	^4F	Co^{3+}	1	10	^5D	−1	−1
Ni^{2+}	3	13	^3F	Ni^{3+}	2	11	^4F	−1	−2
Cu^{2+}	4	16	^2D	Cu^{3+}	3	13	^3F	−1	−3
Zn^{2+}	5	20	^1S	Zn^{3+}	4	16	^2D	−1	−4

Table 3 summarizes numbers of pairing interactions, p_2 and p_3; exchange interactions, e_2 and e_3; changes on ionization, Δp and Δe; and term symbols for doubly and triply charged ions. Figure 11 shows the third ionization energies modified by pairing and exchange energies, $P\Delta p$ and $E_{ex}\Delta e$, so that scandium, vanadium, manganese, iron, nickel, and zinc form a smooth, almost-linear curve with titanium and

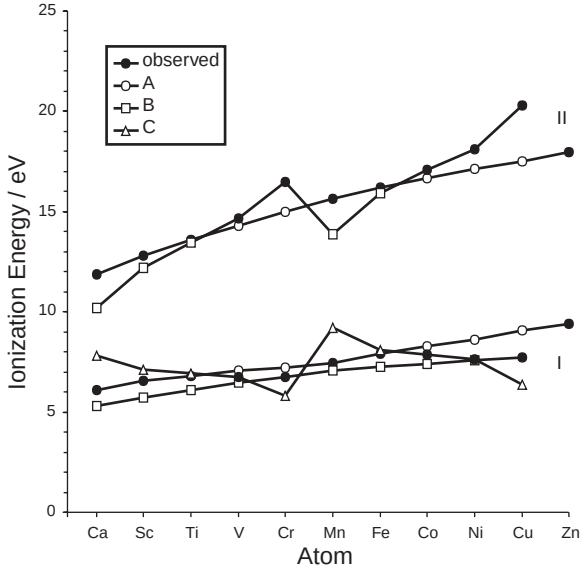

Figure 10. First and second ionization energies of calcium to zinc. Roman numerals denote the ionization number. See text for explanation of the curves A–C.

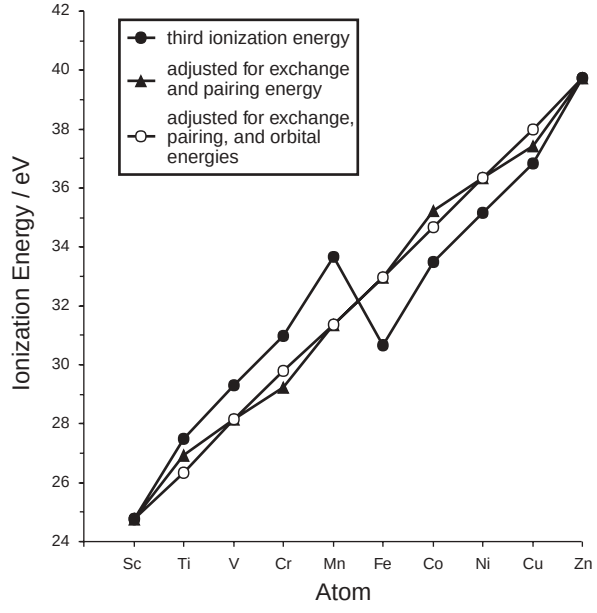

Figure 11. Third ionization energies of scandium to zinc.

cobalt above the curve and chromium and copper below. These irregularities are the result of changes in orbital energy, E_{orb}, since F → D transitions are higher and D → F transitions are lower in energy. Application to titanium, chromium, cobalt, and copper gives a nearly linear curve that increases from scandium to zinc, where $P = {}^{-}4E_{ex} = \pm 4E_{orb} =$ 2.32 eV. Orbital energy changes were not relevant for p electrons and cannot be identified for D → S and S → D transitions involving scandium, manganese, iron, and zinc, the first and last members of each arm of the zigzag pattern.

Fourth ionization energies increase from titanium to iron, decrease to cobalt, and increase to gallium. Similar modification by pairing, exchange, and orbital energies gives an almost linear curve increasing from titanium to gallium, where $P = {}^{-}4E_{ex} = \pm 4E_{orb} = 2.80$ eV.

Second Transition Period

First and second ionization energies of the second transition period are examined in Figure 12. Strontium, zirconium, technetium, and cadmium lose both s electrons in processes $M(4d^n5s^2) \rightarrow M^+(4d^n5s^1) \rightarrow M^{2+}(4d^n5s^0)$. Their ionization energies, with energies derived from wavenumbers of excited states for other atoms *(1)*, fall on curves IA and IIA. Niobium, molybdenum, ruthenium, rhodium, and silver lose one s and then one d electron in the processes $M(4d^{n+1}5s^1) \rightarrow M^+(4d^{n+1}5s^0) \rightarrow M^{2+}(4d^n5s^0)$. Their ionization energies form part of curve IB and of zigzag pattern IIB. Yttrium follows the pathway $M(4d^15s^2) \rightarrow M^+(4d^05s^2) \rightarrow M^{2+}(4d^05s^1)$. The first ionization energy falls near curve IA and the second on IIB. Palladium loses two d electrons in the processes $M(4d^{10}5s^0) \rightarrow M^+(4d^95s^0) \rightarrow M^{2+}(4d^85s^0)$. The first ionization energy falls near curve IA and the second forms part of curve IB. Cadmium (n = 10) does not form part of curve IB or zigzag pattern IIB.

Third ionization energies involve loss of one d electron in $M^{2+}(4d^n5s^0) \rightarrow M^{3+}(4d^{n-1}5s^0)$ transitions. The zigzag pattern in Figure 1, excluding strontium (Z = 38, n = 0), increases from yttrium to technetium, decreases to ruthenium, and increases to cadmium. Modification by pairing, exchange, and orbital energies gives a smooth curve increasing from yttrium through technetium and ruthenium to cadmium, where $P = -4E_{ex} = \pm 4E_{orb} = 1.46$ eV.

Third Transition Period

Barium and lanthanum precede the lanthanides and have lower first ionization energies than other atoms in the third transition period. Hafnium loses one d electron and then loses two s electrons and gains one d electron in the processes $M(5d^26s^2) \rightarrow M^+(5d^16s^2) \rightarrow M^{2+}(5d^26s^0)$. Tantalum and tungsten lose two s electrons and gain one d electron in the process $M(5d^n6s^2) \rightarrow M^+(5d^{n+1}6s^0)$; rhenium, osmium, iridium, and mercury lose one s electron in the process $M(5d^n6s^2) \rightarrow M^+(5d^n6s^1)$; and platinum and gold lose one s electron and then one d electron in the processes $M(4d^{n+1}6s^1) \rightarrow M^+(5d^{n+1}6s^0) \rightarrow M^{2+}(5d^n6s^0)$. Mercury loses two s electrons in the processes $M(5d^{10}6s^2) \rightarrow M^+(5d^{10}6s^1) \rightarrow M^{2+}(5d^{10}6s^0)$.

Rare Earth Metals

Table 4 summarizes outer electronic configurations of atoms and ions from the lanthanum and actinium series *(2–4)*. Eleven pairs of atoms have similar configurations. First ionization energies are plotted in Figure 13 against number of post-lanthanum or post-actinium electrons, n, which represents the position of the atom in the f block. Most actinides have higher ionization energies than corresponding lanthanides.

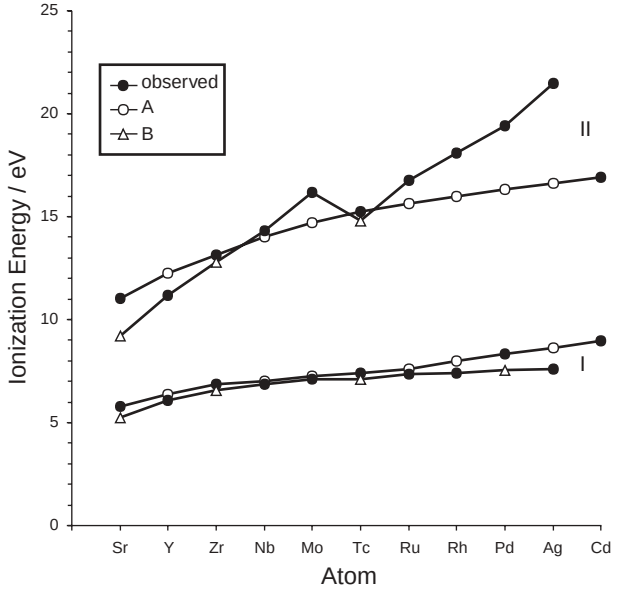

Figure 12. First and second ionization energies of strontium to cadmium. Roman numerals denote the ionization number. See text for explanation of the curves A and B.

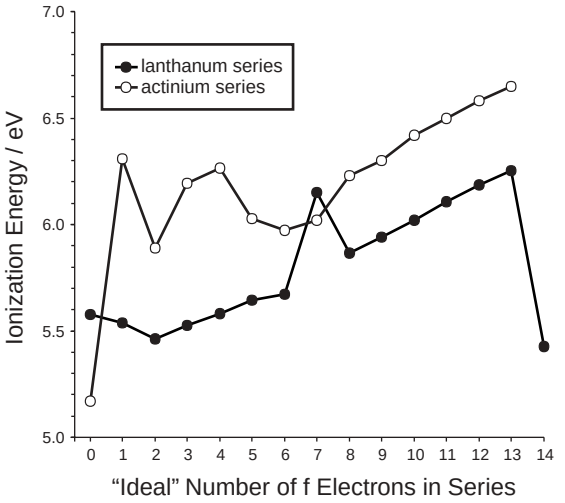

Figure 13. First ionization energies of lanthanum and actinium series.

Table 4. Ground State Electronic Configurations for the Lanthanum and Actinium Series

n	*Z*	Atom	M			M^+			M^{2+}			M^{3+}		
			4f	5d	6s	4f	5d	6s	4f	5d	6s	4f	5d	6s
0	57	La	0	1	2	0	2	0	0	1	0	0	0	0
1	58	Ce	1	1	2	1	2	0	2	0	0	1	0	0
2	59	Pr	3	0	2	3	0	1	3	0	0	2	0	0
3	60	Nd	4	0	2	4	0	1	4	0	0	3	0	0
4	61	Pm	5	0	2	5	0	1	5	0	0	4	0	0
5	62	Sm	6	0	2	6	0	1	6	0	0	5	0	0
6	63	Eu	7	0	2	7	0	1	7	0	0	6	0	0
7	64	Gd	7	1	2	7	1	1	7	1	0	7	0	0
8	65	Tb	9	0	2	9	0	1	9	0	0	8	0	0
9	66	Dy	10	0	2	10	0	1	10	0	0	9	0	0
10	67	Ho	11	0	2	11	0	1	11	0	0	10	0	0
11	68	Er	12	0	2	12	0	1	12	0	0	11	0	0
12	69	Tm	13	0	2	13	0	1	13	0	0	12	0	0
13	70	Yb	14	0	2	14	0	1	14	0	0	13	0	0
14	71	Lu	14	0	2	14	0	2	14	0	1	14	0	0
			5f	6d	7s	5f	6d	7s						
0	89	Ac	0	1	2	0	0	2						
1	90	Th	0	2	2	0	2	1						
2	91	Pa	2	1	2									
3	92	U	3	1	2									
4	93	Np	4	1	2									
5	94	Pu	6	0	2									
6	95	Am	7	0	2									
7	96	Cm	7	1	2									
8	97	Bk	9	0	2									
9	98	Cf	10	0	2									
10	99	Es	11	0	2									
11	100	Fm	12	0	2									
12	101	Md	13	0	2									
13	102	No	14	0	2									
14	103	Lr	14	1	2									

Table 5. Pairing and Exchange Interactions and Term Symbols for Ions of the Lanthanum Series

Ion	p_2	e_2	Term	Ion	p_3	e_3	Term	Δ_p	Δe
La^{2+}	0	0	^2F	La^{3+}	0	0	^1S	0	0
Ce^{2+}	0	1	^3H	Ce^{3+}	0	0	^2F	0	−1
Pr^{2+}	0	3	^4I	Pr^{3+}	0	1	^3H	0	−2
Nd^{2+}	0	6	^5I	Nd^{3+}	0	3	^4I	0	−3
Pm^{2+}	0	10	^6H	Pm^{3+}	0	6	^5I	0	−4
Sm^{2+}	0	15	^7F	Sm^{3+}	0	10	^6H	0	−5
Eu^{2+}	0	21	^8S	Eu^{3+}	0	15	^7F	0	−6
Gd^{2+}	1	21	^7F	Gd^{3+}	0	21	^8S	−1	0
Tb^{2+}	2	22	^6H	Tb^{3+}	1	21	^7F	−1	−1
Dy^{2+}	3	24	^5I	Dy^{3+}	2	22	^6H	−1	−2
Ho^{2+}	4	27	^4I	Ho^{3+}	3	24	^5I	−1	−3
Er^{2+}	5	31	^3H	Er^{3+}	4	27	^4I	−1	−4
Tm^{2+}	6	36	^2F	Tm^{3+}	5	31	^3H	−1	−5
Yb^{2+}	7	42	^1S	Yb^{3+}	6	36	^2F	−1	−6
Lu^{2+}			^2S	Lu^{3+}			^1S		

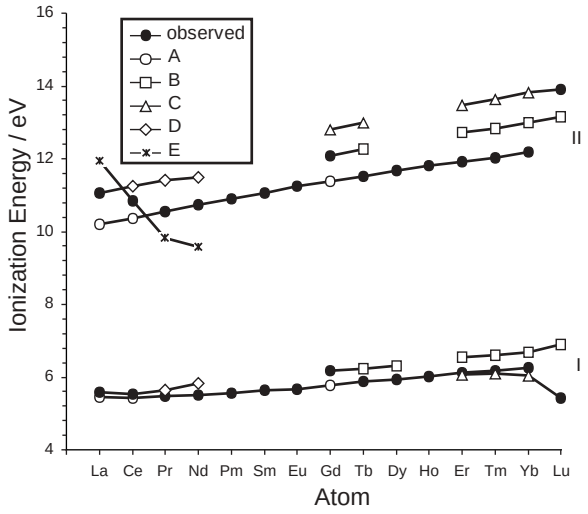

Figure 14. First and second ionization energies of lanthanum series.

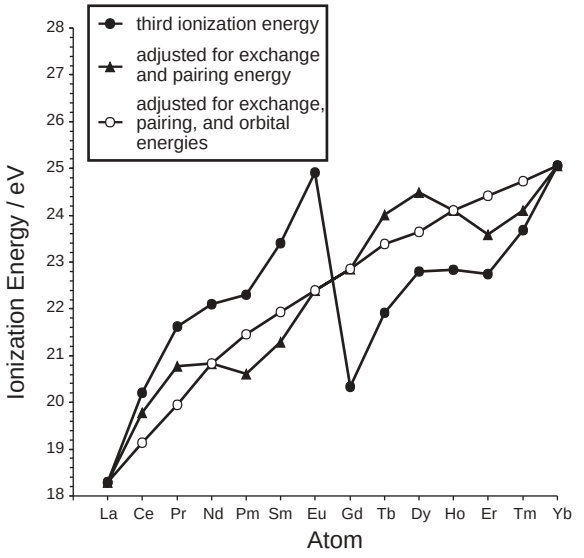

Figure 15. Third ionization energies of lanthanum series.

Lanthanum Series

First and second ionization energies of the lanthanum series are examined in Figure 14. Filled circles represent NBS (National Bureau of Standards) values *(3, 4)*. Other symbols represent ionization energies derived from wavenumbers of excited states for neighboring atoms *(3)*. Most atoms lose both s electrons during processes $M(4f^{n+1}5d^06s^2) \rightarrow M^+(4f^{n+1}5d^06s^1) \rightarrow M^{2+}(4f^{n+1}5d^06s^0)$. Their ionization energies fall on curves IA and IIA with derived energies for lanthanum, cerium, and gadolinium but not lutetium ($n = 14$). Gadolinium loses both s electrons during the processes $M(4f^75d^16s^2) \rightarrow M^+(4f^75d^16s^1) \rightarrow M^{2+}(4f^75d^16s^0)$ and ionization energies fall on curves IB and IIB with energies derived from ref *3* for most atoms from terbium to lutetium. The A and B curves increase across the series and are approximately parallel with differences that might depend on shielding by 6s or 4f electrons.

Lutetium has filled 4f orbitals and loses one d electron followed by one s electron in $M(4f^{14}5d^16s^2) \rightarrow M^+(4f^{14}5d^06s^2) \rightarrow M^{2+}(4f^{14}5d^06s^1)$ transitions. These ionization energies fall on curves IC and IIC (approximately parallel to IIA and IIB) with energies derived from wavenumbers *(3)* for erbium, thulium, and ytterbium. Lanthanum and cerium lose two s electrons and gain one d electron in $M(4f^n5d^16s^2) \rightarrow M^+(4f^n5d^26s^0)$ transitions. Their ionization energies fall on curve ID with derived energies for praseodymium and neodymium. Lanthanum loses secondly one d electron and falls on curve IID with derived energies for cerium, praseodymium, and neodymium. Cerium loses secondly two d electrons while gaining one f electron and forms part of reverse zigzag pattern IIE with derived energies for lanthanum, praseodymium, and neodymium.

Third ionization energies in Figure 15 refer to loss of one f electron in $M^{2+}(4f^{n+1}5d^06s^0) \rightarrow M^{3+}(4f^n5d^06s^0)$ transitions. They increase from lanthanum to praseodymium, flatten to promethium, increase to europium, and decrease to gadolinium with similar behavior from gadolinium to ytterbium giving a distorted zigzag pattern. These energies derived for excited states of lanthanum and gadolinium *(3)* differ slightly from ground-state ionization energies in Figure 1.

Table 5 summarizes numbers of pairing interactions (pairs of electrons occupying the same orbital), p_2 and p_3; numbers of exchange interactions between pairs of electrons having parallel spins, e_2 and e_3; changes on ionization, Δp and Δe; and term symbols for ions of the lanthanide series. Corrections for exchange and pairing energies remove the principal discontinuity but as with d electrons, orbital energies must be considered *(19, 23)*. Corrections involving H → F transitions, E_{orb1}, and I → H transitions, E_{orb2}, and corresponding negative transitions produce a surprisingly smooth curve, where $P = -6E_{ex} = \pm 4E_{orb1} = \pm 3E_{orb2} = 2.625$ eV. Estimated experimental errors for third ionization energies include ±0.4 eV for Pm and ±0.3 eV for Nd, Sm, and Dy *(3)*.

Fourth ionization energies of the lanthanides show a similar distorted zigzag pattern. Fourteen atoms from cerium through lutetium but not lanthanum ($n = 0$), lose one f electron in $M^{3+}(4f^n5d^06s^0) \rightarrow M^{4+}(4f^{n-1}5d^06s^0)$ transitions. Corrections for pairing, exchange, and orbital energies produce a reasonably smooth curve when $P = -6E_{ex} = \pm 4E_{orb1} = \pm 3E_{orb2} = 2.6$ eV, despite estimated experimental errors of ±0.7 eV (Sm and Gd), ±0.6 eV (Pm, Eu, and Ho), and ±0.4 eV (Nd, Dy, Er, and Tm).

Actinium Series

Electronic configurations of lanthanum and actinium are similar for atoms but different for ions, and actinium has the lower ionization energy. An irregular pattern from thorium to neptunium and americium and curium in Figure 13 suggests that cations have different configurations. Ionization energies of plutonium and berkelium to nobelium fall on a smooth curve in the second half of the series that is approximately parallel to the curve from europium to ytterbium and suggests loss of one s electron in $M(5f^{n+1}6d^07s^2) \rightarrow M^+(5f^{n+1}6d^07s^1)$ transitions. We are unable to find a reliable ionization energy for lawrencium.

Conclusion

This paper reviews the ionization energies of atoms and atomic ions in the s, p, d, and f blocks of the periodic table. The apparently irregular behavior of the first and second ionization energies across the transition-metal and rare earth periods is explained in terms of electronic configurations of the atoms and ions. A semiquantitative treatment of pairing energies, P, exchange energies, E_{ex}, and orbital energies, E_{orb}, explains discontinuities at half-filled p, d, and f electron shells.

Some of the great advances of the last century in the understanding of atomic spectra and ionization energies are summarized in the Appendix at the suggestion of a reviewer.

Acknowledgments

We thank C. D. Flint and P. J. Heard for helpful discussions.

Literature Cited

1. Moore, C. E. *Atomic Energy Levels;* NBS Circular 467; U.S. Department of Commerce: Washington DC; (a) 1949; Vol. 1. (b) 1952; Vol. 2. (c) 1958; Vol. 3.
2. Moore, C. E. *Ionization Potentials and Ionization Limits Derived from the Analyses of Optical Spectra;* NSRDS-NBS 34; U.S. Department of Commerce: Washington DC, 1970.
3. Martin, W. C.; Zalubus, R.; Hagan, L. *Atomic Energy Levels–The Rare Earth Elements;* NSRDS-NBS 60; U.S. Department of Commerce: Washington DC, 1978.
4. *Handbook of Chemistry and Physics*, 81st ed.; Lide, D. R., Ed.; CRC: Boca Raton, FL, 2000.
5. Reader, J. *J. Opt. Soc. Am.* 1975, *65*, 638.
6. Reader, J.; Epstein, G. L. *J. Opt. Soc. Am.* 1976, *66*, 590.
7. Gillespie, R. J.; Moog, R. S.; Spencer, J. N. *J. Chem. Educ.* 1998, *75*, 539–540.
8. Ahrens, L. H. *Ionization Potentials;* Pergamon: Oxford, England, 1983.
9. Pilar, F. L. *J. Chem. Educ.* 1978, *55*, 2–6.
10. Rioux, F.; DeKock, R. L. *J. Chem. Educ.* 1998, *75*, 537–539.
11. Lang, P. F.; Smith, B. C. *Inorg. Nucl. Chem. Letters* 1981, *17*, 27–29.
12. Agmon, N. J. *J. Chem. Educ.* 1988, *65*, 42–44.
13. Ali, M. E. S.; Lang, P. F.; Smith B. C. *J. Chem. Soc., Faraday 2* 1984, *80*, 1089–1091.
14. Born, M. (revised Blin-Stoyle, R. J.; Radcliffe, J. M.) *Atomic Physics*, 8th ed.; Blackie: London, 1969; Chapter 6.
15. Smith, D. W. *J. Chem. Educ.* 1975, *52*, 576–577.
16. Condon, E. U.; Shortley, G. H. *Theory of Atomic Spectra;* Cambridge University: Cambridge, 1955; Chapter 7.
17. Atkins, P. J. *Quanta: A Handbook of Concepts*, 2nd ed.; Oxford University: Oxford, England, 1980; p 113.
18. Blake, A. B. *J. Chem. Educ.* 1981, *58*, 393–398.
19. Johnson, D. A. *Some Thermodynamic Aspects of Inorganic Chemistry*, 2nd ed.; Cambridge University: Cambridge, England, 1982; Chapter 6.
20. Cann, P. *J. Chem. Educ.* 2000, *77*, 1056–1061.
21. Lang, P. F.; Smith B. C. *Educ. Chem.* 1986, *23*, 50–53.
22. Catalan, M. A.; Rohrlich, R.; Shenstone, A. G. *Proc. Roy. Soc.* 1954, *221A*, 421–437.
23. Bills, J. L. *J. Chem. Educ.* 1998, *75*, 589–593.
24. Series, G. W. *Spectrum of Atomic Hydrogen;* Oxford University Press: Oxford, England, 1957; Chapter 3.
25. Hertzberg, G. *Atomic Spectra and Atomic Structure*, 2nd ed.; Dover: New York, 1944; Chapter 1.
26. Sanders, J. H. *The Fundamental Atomic Constants;* Oxford University Press: Oxford, England, 1961; Chapter 2.
27. Born, M. (revised Blin-Stoyle, R. J., Radcliffe, J. M.) *Atomic Physics*, 8th ed.; Blackie: London, 1969; Chapter 4.
28. Sommerfeld, A. *Atomic Structure and Spectral Lines;* Methuen: London, 1934; Chapter 2.
29. Heisenberg, W. *Physical Principals of the Quantum Theory;* Dover: New York, 1930.
30. Atkins, P. W. *Molecular Quantum Mechanics;* Oxford University Press: Oxford, England, 1970; Chapter 8.
31. Bethe H. A.; Salpeter, E. E. *Quantum Mechanics of One and Two Electron Atoms;* Plenum: New York, 1977.

Appendix

In the late 19th century, it was shown that atomic spectra consist of discrete lines rather than continuous emission or absorption. Paschen, Bracket, Pfund, and others made notable contributions *(24)*, and Balmer identified four lines as members of a converging series *(25)*. Rydberg discovered the constant that bears his name *(26)*. At the beginning of the 20th century, Bohr proposed that electrons in an atom occupy discrete energy states and that radiation is emitted or absorbed on transition from one discrete (quantum) state to another *(27)*.

The energy change, ΔE, for hydrogen or a hydrogen-like ion is given by the following expression, where R is the Rydberg constant, Z is the atomic number, and n_1 and n_0 are integers:

$$\Delta E = RZ^2\left(\frac{1}{n_1^2} - \frac{1}{n_0^2}\right)$$

Agreement between theory and experiment was well within the limits of error in the measurement of atomic constants at that time. Sommerfeld and others developed general laws of atomic spectroscopy *(28)*.

Further advances came from the development of wave mechanics and matrix mechanics *(29)*. The Schrodinger equation can be solved exactly only for one-electron ions. Approximate methods were used to determine energy levels and ionisation energies in other systems. In 1930, Slater devised an approximate method for estimating the extent to which electrons are shielded from the nucleus *(30)*. He assumed that each electron is situated in the field of an effective nuclear charge, Z^*, and that an effective quantum number, n^*, could be assigned to each electron. The energy required to ionize an electron, I, could be estimated as:

$$I = R\left(\frac{Z^*}{N^*}\right)^2$$

Slater's rules are based on simple assumptions about shielding and effective nuclear charge. They are unable to account for the zigzag patterns of ionization energies illustrated in Figure 1. More sophisticated equations allow ionisation energies in multielectron atoms to be calculated *(31)*.